ORIGINAL RESEARCH

Performance evaluation of low-cost FRP parabolic trough reflector with mild steel receiver

Atul A Sagade[1*], Satish Aher[2] and Nilkanth N Shinde[3]

Abstract

Solar collector and concentrator system can be used for industrial process heat application in various industries. Apart from the low temperature applications, there are several potential fields of application for solar thermal energy at medium-high temperatures (80°C to 300°C). This paper describes the experimental results of the prototype parabolic trough made of fiberglass-reinforced plastic with its aperture area coated by aluminum foil with a reflectivity of 0.86. From Indian conditions, there is a large potential available for low-cost solar-concentrating technologies for domestic as well as industrial process heat applications. This line-focusing parabolic trough with mild steel receiver coated with black proxy material has been tested with and without glass cover. Instantaneous efficiency of 51% and 39% has been achieved with and without glass cover, respectively. Performance evaluation of the prototype system has been done during the months of April and May 2010 at Shivaji University, Kolhapur (16.42°N latitude, 74.13°W longitude). The total cost of the prototype system developed has been calculated as Rs10,000 (US$200).

Keywords: Solar collector, Solar thermal energy, Fiberglass-reinforced plastic, Solar parabolic trough, Renewable energy technology

Background

Kalogirou et al. described a low-cost method for mass production of parabolic surfaces with fiberglass. The article indicates that the accuracy of the parabolic surface depends on the accuracy of the mold, and details of the mold production and the procedure for producing the parabolic surface are presented. The authors used fiberglass of 4-mm (mean value) thickness. The cost of the parabolic surface is US$30/m^2 of aperture area with 90° rim angle [1].

Valan Arasu and Sornakumar explained the design and manufacturing of a smooth 90°-rim-angle fiberglass-reinforced parabolic trough for water-heating application. The total thickness of the parabolic trough is 7 mm. The concave surface where the reflector is fixed is manufactured to a high degree of surface finish. They have found that the standard deviation of the distribution of the parabolic surface errors is 0.0066 radians from the collector performance test according to ASHRAE Standard 93

(1986), which indicates the high accuracy of the parabolic surface [2].

Martinez et al. developed a 2.37-m aperture, 1.14-m-long parabolic trough concentrator with first surface solar mirrors made over floated soda lime glasses with concave geometry and built with 16 mirrors with sizes of 0.3 × 0.6 m. This reflector yields specular reflectance around 86%. The field test of focusing such a concentrator gave a size focus of about 5.08 cm where over 90% of the reflected beam solar irradiance arrived on a simulated pipe receiver with this diameter [3].

Thomas describes a simple welded frame structure for parabolic trough concentrators suitable for developing countries. He conducted static load tests on this structure to study its deflection characteristics under various load conditions. The results show that the slope error of the reflector support corresponding to normal wind loads was found to be within the specified limits, and the structure withstood the load corresponding to extreme wind load conditions [4].

The collector's performance has been tested by Kalogirou according to the ASHRAE Standard 93(1986). The collector's efficiency and incidence angle modifier have

* Correspondence: atulsagade@gmail.com
[1]Solar Thermal Research Laboratory, New Satara College of Engineering & Management (Polytechnic), Korti-Pandharpur, Maharashtra 413304, India
Full list of author information is available at the end of the article

been measured. The test slope and intercept were found to be 0.387 and 0.638, respectively. The author explained that the collector's time constant is less than 1 min and the collector's acceptance angle obtained from the test is ± 0.5°, which in combination with the tracking mechanism maximum error (± 0.2°) implies that the system works continuously at almost maximum possible efficiency [5].

Thomas and Guven have explored and reviewed the design aspects of the structural, optical, and thermal subsystems of parabolic trough concentrators. Existing methods of performance evaluation and techniques to improve their performance were also discussed by the authors [6].

Gong et al. explains that the vacuum solar receiver is the key component of a parabolic trough solar plant, which plays a prominent role in the gross system efficiency. This paper first establishes and optimizes a one-dimensional (1-D) theoretical model using MATLAB program to compute the receiver's major heat loss through glass envelope and then systematically analyzes the major influence factors of heat loss. With the laboratorial steady state test stand, the heat losses of both good vacuum and non-vacuum Sanle-3 receivers were surveyed by the authors. The authors' comparison shows that the original 1-D model agrees with the end-covered test while remarkably deviating from the end-exposed test. The authors also developed a 3-D model by CFD software to further investigate the different heat transfer processes of the receiver's end components [7].

Skeiker explains that the important parameter affecting the performance of a solar collector is its tilt angle with the horizon. This is because the variation of tilt angle changes the amount of solar radiation reaching the collector surface. Skeiker has developed a mathematical model for estimating the solar radiation on a tilted surface and to determine the optimum tilt angle and orientation (surface azimuth angle) for the solar collector in the main Syrian zones on a daily basis as well as for a specific period. The results expose that changing the tilt angle 12 times in a year maintains approximately the total amount of solar radiation near the maximum value that is found by changing the tilt angle daily to its optimum value. This achieves a yearly gain in solar radiation of approximately 30% more than in the case of a solar collector fixed on a horizontal surface [8].

System description

A schematic sketch of the test setup of the constructed parabolic trough concentrator for domestic hot water application is shown in Figures 1 and 2. The test setup was set at the Department of Technology, Shivaji University. It consists of a solar collector, storage tank of 100-L capacity, non-return valves fitted in the pipe line to define the flow direction, and control valve used to
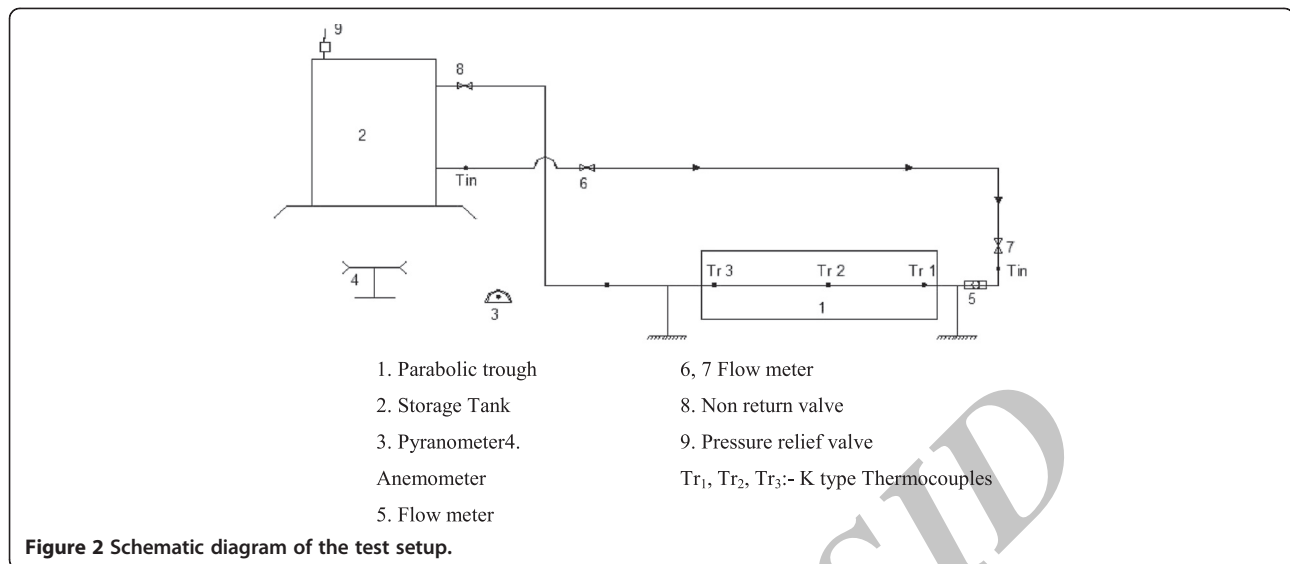

Figure 1 The fiberglass-reinforced plastic parabolic trough.

regulate the flow rate through the circuit. The necessary instruments are attached to the apparatus and then connected to the data acquisition system. For performance evaluation of a system, data collection is important, and for the data collection, measuring instrument is needed. The following instruments were used.

1. Solar radiation: pyranometer (CM6b, Kipp and Zonen, Delft, The Netherlands)
2. Wind Velocity: digital anemometer (AM-4201, Lutron, Taipei, Taiwan)
3. Temperature measurements: set of thermocouple with digital displays.
4. Mass flow rate: flow meter

Fabrication of the fiberglass-reinforced parabolic trough

For construction of the parabolic trough, a composite material is used. E-glass fiberglass-reinforced plastic (FRP) has been selected as material for collector. There are a number of benefits obtained from using FRP composite; these benefits and characteristics were considered during the design and development process. The parabolic trough was constructed by the hand lay-up method. First, the mold was made of a plywood-type wooden material. The accuracy of the fiberglass-reinforced parabolic trough surface depends on the accuracy of the mold; therefore, extreme care has been taken during the construction of the wooden mold. The wooden mold has been constructed with plywood ISI BWR IS 303, which has been manufactured using high-density timber from selected hardwood layers of uniform thickness for good strength and stability. The thickness of the plywood was 20 mm. Firstly, a parabolic rib having a width of 110.23 cm was manufactured. Two parabolic pieces of the same type of were manufactured using a saw machine; these two parabolic pieces were positioned in such a way that the

1. Parabolic trough 6, 7 Flow meter

2. Storage Tank 8. Non return valve

3. Pyranometer4. 9. Pressure relief valve

Anemometer Tr_1, Tr_2, Tr_3:- K type Thermocouples

5. Flow meter

Figure 2 Schematic diagram of the test setup.

space between the adjacent forms on either side is equal. Small recesses were cut on the mold frame to accommodate the parabolic forms, and the parabolic forms were nailed perpendicularly on the mold frame and then connected by means of a wooden strip.

On top of these parabolic forms, a 6-mm smooth-surface plywood was fixed with nails. Wood putty was used to eliminate any marks left by the nails that were polish by sandpaper after the wood putty was set; plane smooth sunmica (a type of smooth plywood) was stuck on the plywood surface with sticky materials (Fevicol, Pidilite, Mumbai, India). A thin film of plastic, 200-μm thick, with size equal to the parabola mold was laid on the wooden parabolic mold. The thin film was used as a release agent and to get a smooth surface inside the parabola. Then, 450-μm chopped strand fiberglass was placed on top of the thin film. The catalyst or Methyl Ethyl Ketone Peroxide Hardener and accelerator cobalt were mixed in polyester resin in a separate bowl. The mixed resin was applied by brushes to the surface of the chopped strand mat, and then, another layer of chopped strand mat was placed on the mixed resin. The fiberglass mat was saturated with the resin by rolling the surface with a brush. The resin was applied on the mat by brushing. A brush was used to work the resin in to the fiber. During the process, extreme care was taken so that the material is securely attached to the mold, and no air is trapped in between the fiberglass and mold. The rolling action of the squeeze assists in removing air bubbles that could prove detrimental to the laminate performance. This process of laying alternate layers of polyester resin and chopped strand fiberglass mat was repeated until a 2-mm-thick fiberglass-reinforced laminate was obtained. Table 1 shows the parameters and dimensions of the terms used in the experimentation.

Methods
Experimental methods
The experiment procedure was started by flushing the system. Then, the system was filled with water and the flow rate was adjusted to the required value. The solar collector was allowed to run for over 20 min to achieve quasi-steady-state conditions before starting the experiments, and the proper working of all measuring instruments was checked, including the connection of the temperature indicator to the temperature sensor, pyranometer, anemometer, and tracking of parabolic trough. Cold water from the storage tank enters the mild steel receiver of the parabolic trough collector. The tank was located above the level of the collector to assure the natural flow of water. As water in the receiver tube, which is located at the focal axis of

Table 1 Parameters and dimensions of terms used in the experimentation

Parameter	Dimension
Aperture of the concentrator (W)	1.10 m
Inner diameter of absorber tube (D_i)	0.020 m
Outer diameter of absorber tube (D_o)	0.025 m
Inner diameter of glass tube	0.050 m
Outer diameter of glass tube	0.056 m
Length of parabolic trough	1.21 m
Concentration ratio	13.69
Collector aperture area	1.33 m^2
Specular reflectivity of concentrator (ρ)	0.85
Glass cover transitivity for solar radiation(τ)	0.85
Absorber tube emissivity/emissivity (a)	0.82
Intercept factor	0.95
Emissivity of absorber tube surface (ε_p)	0.08
Emissivity of glass (ε_c)	0.82

the trough, is heated by solar energy, heated water flows automatically to the top of the water tank and is replaced by cold water from the bottom of the tank. When the water gets heated upon rising to the collector, its density will decrease and the lighter-density water will move up and be stored on top of the storage tank. Higher-density water from the bottom of the tank again enters the parabolic trough and gets heated and moves up and stored in the top of the storage tank. Data of all readings of ambient, fluid, receiver body, and storage tank temperatures and total solar radiations with wind speed every half an hour were collected. The experiment has been performed for 7 h over the day from 0930 hours to 1530 hours. The experiment has been continued with changing input parameters, such as receiver materials and mass flow rate of water.

During the experimentation, a cylindrical parabolic collector has been oriented with its focal axis pointed in the east–west (E-W) orientation so that the focal axis is horizontal. Sun tracking was provided to the parabolic trough collector. Manual tracking was provided to the parabolic trough collector. The trough was rotated about a horizontal (E-W) axis and adjusted manually so that solar beam makes minimum angle of incidence with the aperture plane at all times.

Experimental data collection and calculations
Tables 2 and 3 present the experimental measurements and calculations for the mild steel receiver with and without glass cover, respectively.

Thermal performance calculations
The useful energy delivered from the concentrator can be given by Equations 1 and 2 [9,10]:

$$q_u = mc_p(T_o - T_{in}) \tag{1}$$

$$q_u = mc_p\left[\frac{CS}{U_l} + T_a - T_{in}\right]\left[1 - \exp\left\{-\frac{F^{'}\pi D_o U_l L}{mc_p}\right\}\right] \tag{2}$$

where q_u is the useful energy delivered from the concentrator (W); m, mass flow rate(kg/s); T_o, outlet fluid temperature (°C); T_{in}, inlet fluid temperature (°C); C_p, specific heat of water (kJ/kg°C); C, concentration ratio; S, incident solar flux absorbed in the absorber plate (W/m²); U_l, overall heat loss coefficient (W/m²°C); T_a, ambient temperature (°C); $F^{'}$, collector efficiency factor; D_o, outer diameter of the tube (m); and L is the length of the concentrator (m).

The useful energy gain per unit of the collector length can be expressed by Equations 3 and 4 in terms of the local receiver temperature T_r [1,9,10].

$$q_{u'} = \frac{q_u}{L} \tag{3}$$

$$q_{u'} = \frac{q_u}{L} = F^{'}\left[S - \frac{U_l}{C}(T_r - T_a)\right](W - D_o) \tag{4}$$

where $q_{u'}$ is the useful energy gain per unit of the collector length; T_r, mean receiver surface temperature (°C); W, width of the parabolic reflector (m), and where $F^{'}$ is the collector efficiency factor defined by Equations 5 and 6 [1,5,9,10].

$$F^{'} = 1/U_l\left[\frac{1}{U_l} + \frac{D_o}{D_i h_f}\right] \tag{5}$$

$$q_u = F_R(W - D_o)L\left[S - \frac{U_l}{C}(T_{in} - T_a)\right] \tag{6}$$

where D_i is the inner diameter of the tube (m); h_f, heat transfer coefficient on the inside surface of the tube (W/m²°C); and F_R is the collector heat removal factor.

Heat removal factor is given by Equation 7 [4,9,10],

$$F_R = \frac{mc_p}{\pi D_o L U}\left[1 - \exp\left\{-\frac{F^{'}\pi D_o U_l L}{mc_p}\right\}\right] \tag{7}$$

and collector efficiency can be obtained by dividing q_u by I_b WL. The instantaneous collection efficiency can also be calculated by Equation 8 [9,10]

$$\eta_{in} = \frac{q_u}{I_b r_b WL} \tag{8}$$

where n_{in} is the instantaneous collection efficiency.

Table 2 Experimental measurements and calculation for mild steel receiver without glass cover

Time (hours)	Direct solar radiation on the collector (W/m²)	Wind speed (m/s)	T_{amb} (°C)	T_{in} (°C)	T_{out} (°C)	ΔT (°C)	T_r (°C)	Flux absorbed by the receiver (W/m²)	Useful heat gained by water (W)	Overall heat loss coefficient (W/m²°C)	Instantaneous collector efficiency (%)
0930	667	3.1	29	26	28	02	33	405.5	362.7	44.0	39
1030	861	5.1	31	27	30	03	38	523.4	458.9	44.4	40
1130	977	3.8	34	28	36	08	45	594.0	529.7	49.1	40
1230	1004	6.2	36	29	41	12	49	610.4	457.2	44.1	41
1330	949	5.3	36	30	40	10	54	576.9	493	50.5	39
1430	841	3.5	35	30	39	09	53	511.3	431.1	52.8	37
1530	783	5.2	34	30	32	02	48	476.0	378.0	58.2	36

Mass flow rate, 0.023 kg/s. T_{amb}, ambient temperature; T_{in}, inlet fluid temperature; T_{out}, outlet fluid temperature; ΔT, temperature gradient; T_r, receiver temperature.

Table 3 Experimental measurements and calculation for mild steel receiver with glass cover

Time (hours)	Direct solar radiation on the collector (W/m²)	Wind speed (m/s)	T_{amb} (°C)	T_{in} (°C)	T_{out} (°C)	ΔT (°C)	T_r (°C)	Flux absorbed by the receiver (W/m²)	Useful heat gained by water (W)	Overall heat loss coefficient (W/m²°C)	Instantaneous collector efficiency (%)
0930	696	3.2	29	27	34	07	45	400.8	468.2	18.4	50
1030	764	2.8	32	28	42	14	52	440.0	530.9	12.2	52
1130	793	5.3	36	28	48	20	56	456.7	544.5	16.2	51
1230	928	3.2	38	29	60	31	69	534.5	649.0	11.6	52
1330	976	2.1	39	29	67	38	75	562.1	704.6	8.9	54
1430	899	5.2	39	30	57	27	68	517.8	629.7	12.3	52
1530	812	6.3	34	30	52	22	61	467.7	558.6	14.1	51
1600	764	5.9	33	31	39	08	49	410.9	487.0	20.5	47

Mass flow rate, 0.023 kg/s. T_{amb}, ambient temperature; T_{in}, inlet fluid temperature; T_{out}, outlet fluid temperature; ΔT, temperature gradient; T_r, receiver temperature.

Overall loss coefficient and heat correlations

The calculations of overall loss coefficient were based on convection and re-radiation losses. Heat loss rate per unit length can be given by Equations 9 and 10 [1,5,9,10]:

$$\frac{q_l}{L} = h_{pc}(T_r - T_c)\pi D_o + \sigma \pi D_o (T_r^4 - T_c^4)/\left\{\frac{D_o}{\frac{1}{\varepsilon_p} + D_{ci}\left(\frac{1}{\varepsilon_c} - 1\right)}\right\} \quad (9)$$

$$\frac{q_l}{L} = h_w (T_c - T_a)\pi Dco + \sigma \pi Dco \varepsilon c (T_r^4 - T_a^4) \quad (10)$$

where T_c is the temperature of the cover; h_w, wind heat transfer coefficient(W/m²-K); ε_p, emissivity of absorber surface for long-wavelength radiation; and ε_c, emissivity of the cover for long-wavelength radiation.

Heat transfer coefficient between the absorber tube and the cover

The heat transfer coefficient h_{pc} for the enclosed annular space between a horizontal absorber tube and a concentric cover is calculated by Equations 11, 12, and 13 [9,10]:

$$\frac{K_{eff}}{k} = 0.317 (Ra^*)^{0.25} \quad (11)$$

$$(Ra^*)^{0.25} = \frac{\ln\left(\frac{D_{ci}}{D_o}\right)}{b^{0.75}\left(\frac{1}{D_o^{0.6}} + \frac{1}{D_{ci}^{0.6}}\right)} Ra^{0.25} \quad (12)$$

where Ra* is Rayleigh's number.

Thus,

$$h_{pc} = \frac{2K_{eff}}{D_o \times ln\left(\frac{D_{ci}}{D_o}\right)}. \quad (13)$$

Heat transfer coefficient on the inside surface of the absorber tube

The convective heat transfer coefficient h_f on the inside surface of the absorber tube can be calculated. For Reynolds number greater than 2,000, the flow is turbulent and the heat transfer coefficient may be calculated from Equation 14 [9,10]:

$$Nu = 0.023 Re^{0.8} P_r^{0.4} \quad (14)$$

Results and discussion

Figure 3 shows the variation of inlet and outlet temperatures of the water. The trend explains that, as solar radiation on the receiver enhances, outlet water temperature increases. In comparison, the receiver with glass cover yields much higher outlet water temperature than the receiver without glass cover. The glass cover over the mild steel receiver acts as an insulator, and outlet water temperature and temperature gradient between inlet and outlet water rise sharply. It has been observed that, with glass cover, outlet water temperature and temperature gradient increase by 29% and 68%, respectively.

Figure 4 explores the variation of receiver temperature. From Figure 4, it is clear that the receiver temperature increases with increase in solar radiation. When the receiver is exposed to atmosphere, there are heavier convective heat losses from the receiver as compared to the receiver with glass cover. As said earlier, the glass cover acts as an insulator and also helps in concentrating more solar radiation at the receiver. It has been observed that, with glass cover, receiver temperature has been increased by 23%, which assures hotter water temperature at the outlet.

Figure 5 indicates useful heat gained by the water flowing through the receiver throughout the day. Useful heat gained by the water is affected by various parameters such as wind speed, receiver temperature, and solar radiation. Receiver temperature is the average of three
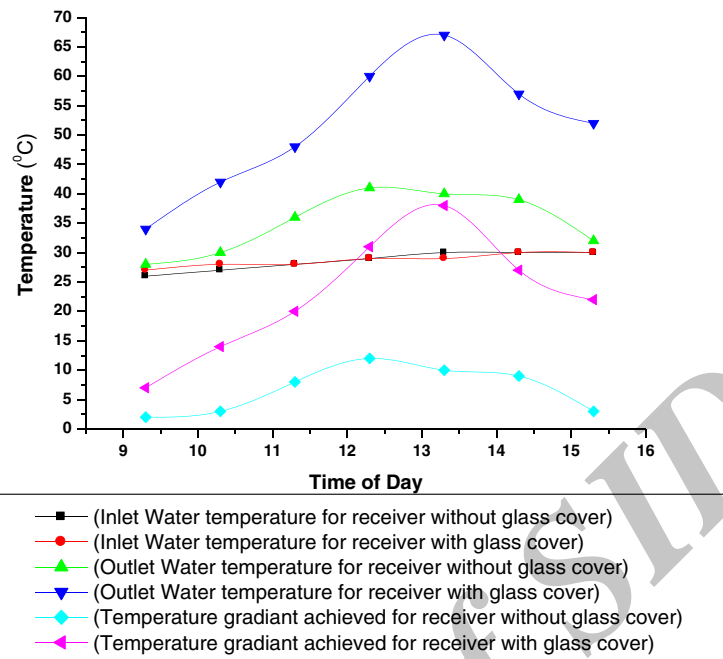
Figure 3 Variation of temperatures throughout the day.

values over the space and not over the time. Temperature was measured at four locations over the length of the receiver. This plotted variation shows that as the receiver surface temperature increases, it increases the thermal conductivity of the air surrounding the receiver. When air conductivity increases, heat losses also increase, but this is not the only cause of heat loss. Figure 5 shows

that, with glass-covered receiver, it is possible to achieve more useful heat gain. It has been observed that as the beam solar radiation incident on the collector increases, more optical energy is captured by the receiver. Compared to the decrease in solar radiation and wind velocity by 4% and 7%, respectively, useful heat gained by the receiver with glass cover increases by 22%
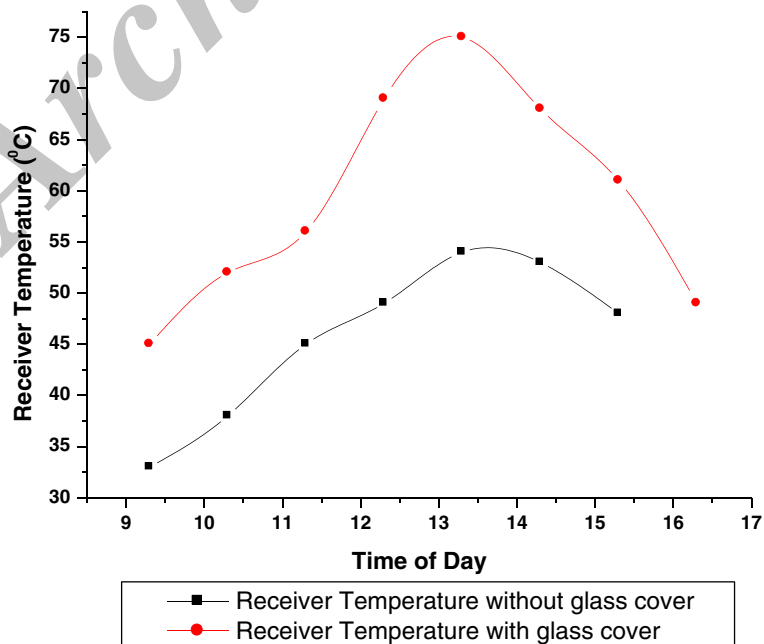
Figure 4 Variation of receiver temperature throughout the day.
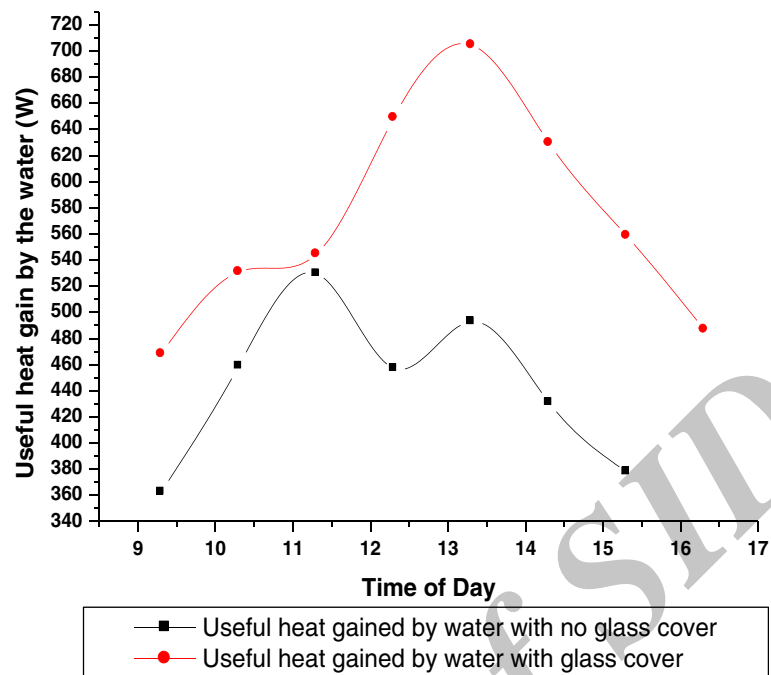
Figure 5 Variation of useful heat gained by water throughout the day.

throughout the day, and average receiver temperature increased by 23%.

Figure 6 explains the variation of collector efficiency and convective heat loss coefficient. The higher the wind speed, the higher will be the convective heat loss and the lower will be the collector efficiency at an instant. It has been observed that the average decrease in heat loss coefficient is 70% when the receiver was covered with glass. When the heat loss coefficient decreased by 70%, the instantaneous efficiency of the collector still increased
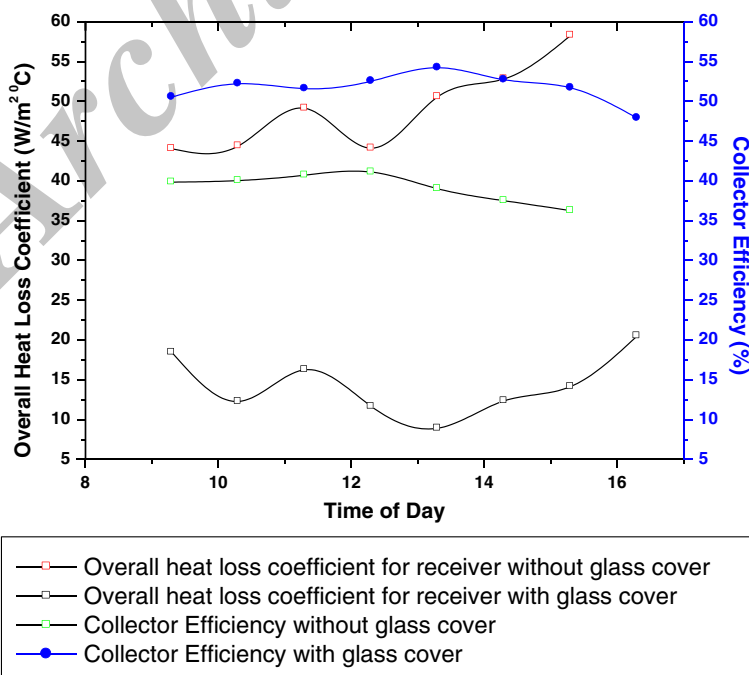
Figure 6 Variation of overall heat loss coefficient and collector efficiency throughout the day.

by 13% with the glass-covered receiver. Instantaneous efficiency of 51% has been achieved with the glass-covered receiver. Radiative heat losses are very small, so their effect on collector efficiency is very small. The main cause for heat loss is temperature gradient between the receiver and surrounding and wind velocity at an instant which therefore increase convective and radiative heat losses from the receiver. An average receiver temperature has been determined to provide accurate receiver loss predictions. Also, wind velocity affects the variation of convective heat loss coefficient. This heat loss also depends upon solar radiation at an instant.

Conclusions

From Indian conditions, low-cost FRP parabolic trough system can prove to be beneficial for industrial heating applications as well as domestic heating. With the system described in this paper, the following conclusions are drawn:

1. Instantaneous efficiency of the collector has been increased by 13%. Instantaneous efficiency of 51.67% has been achieved with the glass-covered receiver.
2. Useful heat gained by the receiver increases by 22% with the glass-covered receiver throughout the day, and the average receiver temperature increased by 23%.
3. It has been observed that, with glass-covered receiver, outlet water temperature and temperature gradient increase by 29% and 68%, respectively.
4. It has been observed that the average decrease in heat loss coefficient is 70% when the receiver was covered with glass.

Competing interests
The authors declare that they have no competing interests.

Authors' contributions
AS and SA carried out all the computations and system designing and drafted the manuscript. NS conceived of the study and participated in its design and coordination. All authors read and approved the final manuscript.

Authors' information
AS, M. Tech, Principal at New Satara College of Engineering & Management, Head of Solar Thermal Research Lab, is involved in research and development programs of solar thermal energy technology in Maharashtra, India, with more than 6 years of experience in the field of solar thermal energy. He was also invited as a solar expert for IEA workshops on the road map of solar heating and cooling at Germany, China, and Australia. SA, M. Tech in Energy, is working as a lecturer at the Amrutvahini College of Engineering and is involved in research activities in the field of thermal energy technology at Shivaji University, Kolhapur, Maharashtra, India. NS, a coordinator and associate professor at the Department of Energy Technology, has 30 years of experience in the field of energy-related issues. He is involved in various energy research projects of the Department of Technology at Shivaji University, Kolhapur, Maharashtra, India. He has more than 150 publications under his name.

Author details
[1]Solar Thermal Research Laboratory, New Satara College of Engineering & Management (Polytechnic), Korti-Pandharpur, Maharashtra 413304, India. [2]Amrutvahini College of Engineering, Sangamner, Maharashtra 422608, India. [3]Department of Energy Technology, Shivaji University, Kolhapur, Maharashtra 416004, India.

References
1. Kalogirou, S, Eleftheriou, P, Lloyd, S, Ward, J: Low cost high accuracy parabolic troughs construction and evaluation. Renew. Energy. **5**(4), 384–386 (1994)
2. Valan Arasu, A, Sornakumar, T: Design, manufacture and testing of fiberglass reinforced parabola trough for parabolic trough solar collectors. Sol. Energy. **81**(10), 1273–1279 (2007)
3. Martinez, I, Almanza, R, Mazari, M, Correa, G: Parabolic trough reflector manufactured with aluminum first surface mirrors thermally sagged. Sol. Energ. Mat. Sol. C. **64**(1), 85–96 (2000)
4. Thomas, A: Simple structure for parabolic trough concentrator. Energ. Convers. Manage. **35**(7), 569–573 (1994)
5. Kalogirou, S: Parabolic trough collector system for low temperature steam generation: design and performance characteristics. Appl. Energ. **55**(1), 1–19 (1996)
6. Thomas, A, Guven, HM: Parabolic trough concentrators—design, construction and evaluation. Energ. Convers. Manage. **34**(5), 401–416 (1993)
7. Gong, G, Huang, X, Wang, J, Hao, M: An optimized model and test of the China's first high temperature parabolic trough solar receiver. Sol. Energy. **84**(12), 2230–2245 (2010)
8. Skeiker, K: Optimum tilt angle and orientation for solar collectors in Syria. Energ. Convers. Manage. **50**(9), 2439–2448 (2009)
9. Duffie, J, Beckman, W: Solar Engineering of Thermal Processes. Wiley, New York (2006)
10. Yogi Goswami, D, Kreith, F, Kreider, JF: Principals of Solar Engineering. Taylor and Fancis, Philadelphia (2003)